Incomplete collisions of wavelength-division multiplexed dispersion-managed solitons

Mark J. Ablowitz, Gino Biondini,* and Eric S. Olson

Department of Applied Mathematics, University of Colorado, Campus Box 526, Boulder, Colorado 80309-0526

Received July 14, 2000; received December 4, 2000

Interactions of wavelength-division multiplexed (WDM) dispersion-managed solitons solitons are studied by means of numerical simulations of both the nonlinear Schrödinger (NLS) equation and the nonlocal equation of the NLS type that describes pulse dynamics in systems with strong dispersion management. The interaction properties are found to depend significantly on the values of system parameters. Incomplete collisions can be particularly serious, because in some parameter regimes they lead to large timing and frequency shifts and in some cases to pulse collapse. However, for parameter values derived from recent experiments with dispersion-managed WDM soliton transmission, the interaction properties are even more favorable than for pure NLS equations. © 2001 Optical Society of America

OCIS codes: 060.5530, 060.4370, 060.4510, 060.4230

1. INTRODUCTION

The use of dispersion management has had a profound influence on long-haul soliton transmission systems. The potential of dispersion-managed (DM) solitons was recently demonstrated by transmission experiments at ultrahigh capacities.[1–3] A key ingredient in these experiments is the simultaneous use of dispersion management and wavelength-division multiplexing. Recently, considerable study has been devoted to understanding the properties of DM solitons and their interactions (see, e.g., Refs. 4 and 5 and references therein). Some of these properties are quite remarkable; for example, dispersion management was shown to yield a reduction of more than an order of magnitude in the collision-induced frequency shifts in wavelength-division multiplexed (WDM) transmission systems.[6–8]

From a theoretical point of view, the properties of DM solitons result from the fact that the introduction of dispersion management into the underlying equations of motion dramatically alters their structure, thereby generating a strikingly different type of behavior. Indeed, in a recent Letter, Ablowitz and Biondini[9] showed that the dynamics in systems with strong dispersion management has multiscale structure and is governed by a nonlocal equation of the nonlinear Schrödinger (NLS) type, which we call the dispersion-managed NLS (DMNLS) equation. Here we use this result to identify the parameters that determine the properties of DM solitons and we study the interaction properties of WDM DM solitons by using both the NLS and the DMNLS equations. The two equations yield consistent results: With either model we find that, in certain parameter regimes and for small enough frequency separation (or, equivalently, small enough relative velocity), DM solitons can exhibit significant nonadiabatic interaction effects. The effects are particularly dramatic for incomplete (that is, partial) collisions. In this case our findings indicate that, below a certain threshold, the two pulses can actually annihilate each other, a phenomenon that is referred to as collapse. These results complement recent studies of partial collisions[10,11] and collisions at zero average dispersion.[12] For parameter values related to recent WDM experiments[2,3] (hereafter, the NEC experiments), however, the previous effects disappear and the interaction properties of the pulses are in some cases even more favorable than for the pure NLS equation.

2. PRELIMINARIES, NORMALIZATIONS, AND UNITS

The evolution of the envelope of a weakly nonlinear quasimonochromatic light pulse in an optical transmission link is described by a perturbed NLS equation:

$$i u_z + (1/2)\, d(z/z_a) u_{tt} + g(z/z_a)|u|^2 u = 0. \qquad (1)$$

The dimensionless variables t, z, d, and u are related to the corresponding quantities in the laboratory frame by $z = z_{\mathrm{lab}}/z_{\mathrm{NL}}$, $t = t_{\mathrm{ret}}/t_*$, $d = -k''/k''_*$, and $u = E/\sqrt{g(z)P_*}$, where E is the field envelope in physical units, z_{NL} is the nonlinear length of the pulse, and P_* is the pulse peak power.[13] Once t_* is fixed, $k''_* = t_*^2/z_{\mathrm{NL}}$ follows as a constraint. Two alternative choices for t_* are $t_* = \tau_{\mathrm{FWHM}}$ (the full width at half-maximum) and, if $\langle k'' \rangle \neq 0$, $t_* = \tau_{\mathrm{NL}}$, with $\tau_{\mathrm{NL}} = \sqrt{\langle k'' \rangle z_{\mathrm{NL}}}$. Hereafter, the angle brackets $\langle\,\rangle$ denote the average over one period of the dispersion map.

The functions $d(\,)$ and $g(\,)$ represent the local value of fiber dispersion and the periodic power variation that is due to loss and amplification, respectively[13]; z_a denotes the dimensionless distance between amplifiers, which we take to coincide with the period of the dispersion map. If erbium-doped fiber amplifiers are used, $g(z) = g_0 \exp[-2\Gamma(z - nz_a)]$ for $nz_a \leqslant z < (n+1)z_a$, where $g_0 = 2\Gamma z_a/[1 - \exp(-2\Gamma z_a)]$ and Γ is the dimensionless loss coefficient. The pure NLS case is obtained for $g(\,) = |d(\,)| = 1$.

0740-3224/2001/050577-07$15.00

Throughout this study, we fix our units by using values derived from the two NEC experiments,[2,3] with which error-free transmission was achieved at 1.1 Tbits/s (55 WDM channels at 20 Gbits/s, each with 0.8-nm channel spacing) over 3020 km and 3.2 Tbits/s (160 WDM channels at 20 Gbits/s each with 0.4-nm channel spacing) over 1500 km, respectively. The relevant pulse parameters for normalization purposes are $P_* = 1\,\mathrm{mW}$, $z_{\mathrm{NL}} = 465\,\mathrm{km}$, and $\langle k'' \rangle = -0.10\,\mathrm{ps}^2/\mathrm{km}$, with $\tau_{\mathrm{FWHM}} = 18\,\mathrm{ps}$ (estimated) at the chirp-free point in the anomalous fiber section. If amplifiers are placed 50 km apart as in the NEC experiments, $z_a = 0.11$ in the above units and $\Gamma = 10.6$ for 0.20-dB/km loss.

3. STRONGLY DISPERSION-MANAGED SYSTEMS

One can conveniently study strong dispersion management by decomposing the dispersion coefficient as[9] $d(z/z_a) = \langle d \rangle + (1/z_a)\Delta(z/z_a)$, where $\Delta(z/z_a)$ has a zero average. In terms of physical quantities, $\langle d \rangle = -\langle k'' \rangle / k''_*$ and $\Delta(\,) = -z_a(k'' - \langle k'' \rangle)/k''_*$. We consider a symmetric two-step dispersion map as the periodic extension of $\Delta(\zeta) = \Delta_1$ for $0 \leqslant |\zeta| < \theta/2$ and $\Delta(\zeta) = \Delta_2$ for $\theta/2 < |\zeta| < 1/2$, where $\zeta = z/z_a$ and θ is a parameter that fixes the length of the first fiber segment as θ_{z_a} (thus, $0 \leqslant \theta \leqslant 1$).

With these assumptions, a multiscale analysis of Eq. (1) shows that,[9] to leading order in z_a, the solution of NLS equation (1) can be written as

$$\hat{u}(z, \omega) = \hat{U}(z, \omega)\exp[-iC(z/z_a)\omega^2/2], \tag{2}$$

with $C'(\zeta) = \Delta(\zeta)$ and $\hat{u}(z, \omega) = \mathcal{F}_\omega[u(z, t)]$, where $\mathcal{F}_{\omega_1, \ldots, \omega_n}[\,]$ represents the n-dimensional Fourier transform; and that $\hat{U}(z, \omega)$ satisfies the DMNLS equation (see also Ref. 14), written either in the time or in the Fourier domain:

$$iU_z + (1/2)\langle d \rangle U_{tt} + \int\int_{-\infty}^{+\infty} dt'dt''U(z, t + t') \times U(z, t + t'')U^*(z, t + t' + t'')R_s(t't'') = 0, \tag{3}$$

$$i\hat{U}_z - (1/2)\langle d \rangle \omega^2 \hat{U} + \int\int_{-\infty}^{+\infty} d\omega' d\omega'' \hat{U}(z, \omega + \omega') \times \hat{U}(z, \omega + \omega'')\hat{U}^*(z, \omega + \omega' + \omega'')r_s(\omega'\omega'') = 0, \tag{4}$$

respectively, with $r_s(x) = \langle g(\zeta)e^{[iC(\zeta)x]} \rangle / 4\pi^2$ and $R_s(tt') = 2\pi\mathcal{F}^{-1}_{t,t'}[r_s(\omega\omega')]$. The DMNLS equation is the fundamental equation that governs the evolution of an optical pulse in a strongly dispersion-managed system. It applies equally well to describing pulse evolution with anomalous, zero, or normal values of average dispersion. In what follows, we shall use the kernels for a lossless two-step map:[9]

$$r_s(x) = \sin(sx)/4\pi^2 sx, \tag{5a}$$

$$R_s(tt') = \mathrm{ci}(|tt'/s|)/2\pi|s|. \tag{5b}$$

where $\mathrm{ci}(x) = \int_1^\infty \mathrm{d}y\, \cos(xy)/y$ is the cosine integral and

$$s = [\theta\Delta_1 - (1 - \theta)\Delta_2]/4. \tag{6}$$

In general, the values of s and $\langle d \rangle$ depend on the arbitrary constant, t_*. However, if $\langle k'' \rangle \neq 0$ it is possible to perform a rescaling of the independent variables in Eq. (3) such that only the ratio $s/\langle d \rangle$ appears in the equation. Alternatively, the same result can be obtained by proper choice of t_* (see next paragraph). Therefore, if $\langle k'' \rangle \neq 0$, the properties of DM solitons are determined not by the individual values of s and $\langle d \rangle$ but only by the sign of $\langle k'' \rangle$ and by the modified map strength:

$$M = s/|\langle d \rangle| = [(k''_1 - \langle k'' \rangle)L_1 - (k''_2 - \langle k'' \rangle L_2]/4|\langle k'' \rangle| z_{NL}. \tag{7}$$

For comparison purposes, we recall the usual definition of map strength:[15,16]

$$S = [(k''_1 - \langle k'' \rangle)L_1 - (k''_2 - \langle k'' \rangle)L_2]/\tau^2_{\mathrm{FWHM}}. \tag{8}$$

It is important to note that M and S are two complementary measures of map strength because M does not depend on the pulse width and S does not depend on the pulse power. Choosing $t_* = \tau_{\mathrm{FWHM}}$ implies $s = S/4$ and $\langle d \rangle = -\langle k'' \rangle z_{\mathrm{NL}}/\tau^2_{\mathrm{FWHM}}$, whereas choosing $t_* = \sqrt{\langle k'' \rangle z_{\mathrm{NL}}}$ yields $s = M$ and $\langle d \rangle = -\mathrm{sgn}\langle k'' \rangle$. In either case, however, M follows naturally from Eq. (3) if $\langle k'' \rangle \neq 0$.

From here on we use the latter definition of t_*, that is, we choose $t_* = \tau_{\mathrm{NL}} = 6.8\,\mathrm{ps}$, and we restrict ourselves to the case $\langle k'' \rangle < 0$, which yields $\langle d \rangle = 1$. For equal-length fiber segments (that is, for $\theta = 1/2$) and with the parameter values fixed in Section 2, Eq. (7) yields the fiber dispersion coefficients in dimensional units as $\Delta D = 72.7\, M\langle D \rangle$. For a typical value of $\langle k'' \rangle = -0.10\,\mathrm{ps}^2/\mathrm{km}$ we have $\langle D \rangle = 0.078\,(\mathrm{ps/nm})/\mathrm{km}$, which yields $\Delta D = 5.67\, M\,(\mathrm{ps/nm})/\mathrm{km}$.

4. DISPERSION-MANAGED SOLITONS

DM solitons correspond to the traveling-wave solutions of the DMNLS equation. Stationary solutions of DMNLS equations can be written as $U(z, t) = f(t)\exp(i\lambda^2 z/2)$, where $F(\omega) = \mathcal{F}_\omega[f(t)]$ is a solution of the following nonlinear eigenvalue problem:[9]

$$(\lambda^2 + \omega^2)F(\omega) = 2\int\int_{-\infty}^{+\infty} d\omega' d\omega'' F(\omega + \omega')F(\omega + \omega'') \times F^*(\omega + \omega' + \omega'')r_M(\omega'\omega''). \tag{9}$$

Given the eigenvalue λ and the reduced map strength M, this nonlinear integral equation can readily be solved numerically with a modified Neumann iteration procedure.[17,18] As the DMNLS equation is invariant under Galilean transformations, one can obtain all traveling-wave solutions by applying a Galilean boost to the stationary solutions:

$$V(z, t) = U(z, t - \Omega_z)\exp(i\Omega t - i\Omega^2 z/2), \tag{10}$$

where Ω is the dimensionless frequency offset. For small values of z_a, these solutions are good approximations to the profile of the breathing solutions of Eq. (1) sampled at

the chirp-free location in the anomalous fiber segment. More details about the comparison between solutions of the DMNLS equation and solutions of the original Eq. (1) are contained in Ref. 18.

For the pure NLS equation (i.e., when $M = 0$) we have the familiar solution $f(t) = \lambda \operatorname{sech}(\lambda t)$. Thus, for pure NLS equations, the eigenvalue λ coincides with the pulse amplitude (that is, $|U|_{\max} = \lambda$), is directly proportional to the pulse energy $\|U\|^2 = \int dt |U(z,t)|^2 = \|u\|^2$, and is inversely proportional to the pulse width $\tau_{\mathrm{rms}}^2 = 4 \int dt\, t^2 |U(z,t)|^2 / \|U\|^2$. More precisely, $\|u\|_{\mathrm{NLS}}^2 = 2\lambda$ and $\tau_{\mathrm{rms,NLS}} = \pi/\sqrt{3}\lambda$.

In the more general DM case ($M \neq 0$), the previous simple proportionality relations of eigenvalue λ with the pulse parameters are lost. However, for any fixed M, the value of λ uniquely determines all relevant pulse parameters such as energy $\|u\|^2$, width τ_{rms}, and expansion factor E, defined as the ratio of maximum to minimum pulse width within the dispersion map (cf. Refs. 18 and 19). When necessary, we use the pulse energy to fix the value of λ to match a given experimental configuration.

5. NUMERICAL ISSUES

To study WDM interactions we integrated both the NLS equation (1) with loss, amplification, and dispersion management (by using a second-order split-step method), and the (lossless) DMNLS equation in the Fourier domain [Eq. (4)]. The double integral in Eq. (4) was discretized with a fourth-order quadrature scheme, and the resultant coupled ordinary differential equations are integrated with a fourth-order Runge–Kutta algorithm.

We should emphasize that, although the numerical integration of the DMNLS equation can be computationally intensive, the equation is quite useful because it provides a reduced model that retains the core features of DM solitons while eliminating the complications that result from the fast dynamics (internal breathing, chirp-free positioning, etc.) and it eliminates the need for ultrawide spatiotemporal integration windows that otherwise would be necessary (for properly accommodating the large relative zigzags of the pulses) when one is using the full NLS equation to simulate WDM interactions with large map strengths and realistic values of channel separation.

In all the cases that we studied, numerical integrations of the lossless DMNLS equation were tested against numerical simulations of the full NLS equation with loss–amplification and dispersion management. Although the details of the simulations differ slightly in cases of collapse, we found that the two models are in remarkable agreement, which means that the DMNLS equation captures all the relevant features of the interactions between dispersion-managed solitons. Accordingly, all the collision cases presented here can be interpreted either as the solution of the DMNLS equation or as the solution of the NLS equation sampled stroboscopically at the chirp-free location in the anomalous fiber section of each dispersion map.

In all the figures presented here one can find the values of time and distance in laboratory units by multiplying the dimensionless values by the corresponding time and length units t_* and z_* introduced in Sections 2 and 3. We also note that, in general, the simulations were run to whatever distance was necessary to complete the interaction; for any given case, this distance depends on the frequency separation of the two pulses as well as on the strength of the interaction.

6. INTERACTIONS OF DISPERSION-MANAGED SOLITONS

Let us start by briefly reviewing the interaction properties of classical solitons of the NLS equation. Inasmuch as the one-dimensional NLS equation is an integrable system, interactions between classical NLS solitons are always elastic. The timing shift that is due to interaction between two WDM solitons can be computed by inverse-scattering methods, and it is possible to obtain a complete characterization of the WDM interactions by using a suitable asymptotic expansion of the exact N-soliton solution of the NLS equation.[20] During the collision, the solitons experience a temporary frequency shift, and they generate a small four-wave mixing contribution that is then reabsorbed into the solitons after the collision. However, when loss and amplification are taken into account, integrability is lost; a residual frequency shift[21] and the resonant four-wave mixing components[22,23] remain after the collision is completed.

We now discuss WDM interactions between DM solitons. We carried out simulations over a wide region of the relevant parameter space (which includes map

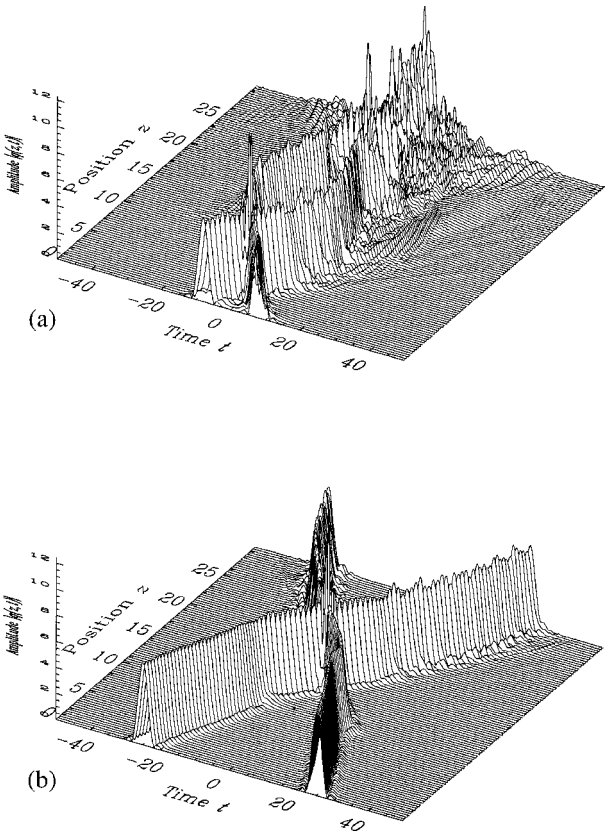

Fig. 1. Collisions between two DM solitons with $M = 10$, $\lambda = 5$ (corresponding to $\|u\|^2 = 94.3$), and $\Delta\Omega = 3.75$: (a) incomplete collision, initial separation $\Delta t_0 = 16$; (b) complete collision, $\Delta t_0 = 50$.

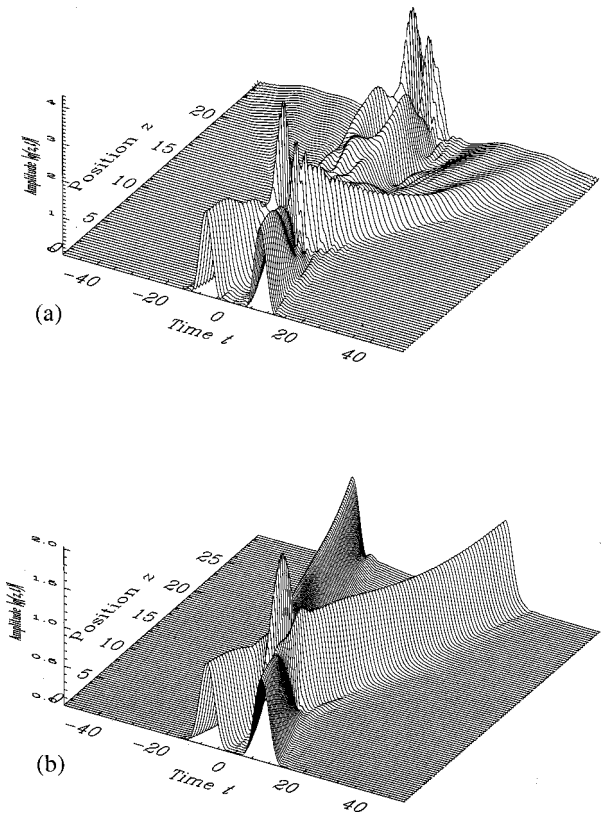

Fig. 2. Incomplete collisions of two DM solitons with $M = 10$, $\Delta\Omega = 2$, and $\Delta t_0 = 16$: (a) $\lambda = 2$, yielding $\|u\|^2 = 15.58$; (b) $\lambda = 1$, yielding $\|u\|^2 = 4.276$.

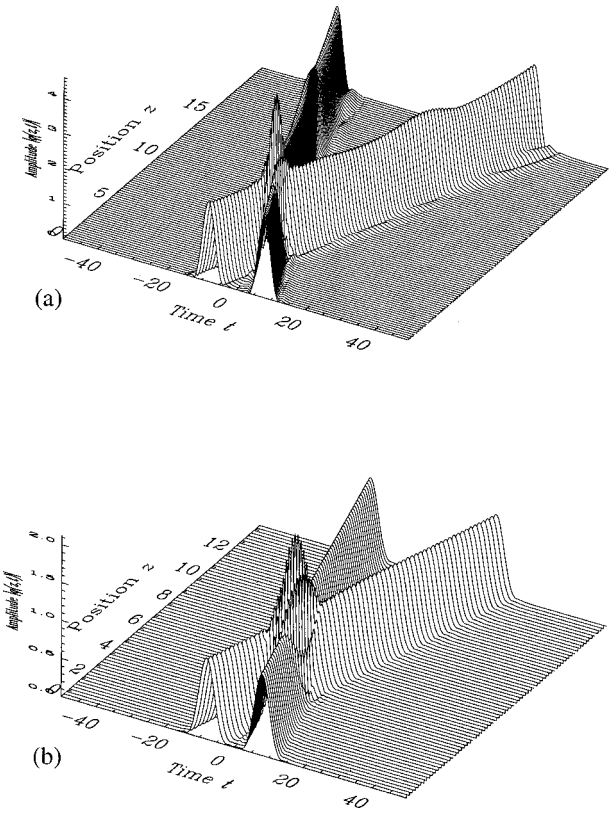

Fig. 3. Incomplete collisions of two DM solitons with $M = 10$, $\Delta\Omega = 3.75$, and $\Delta t_0 = 16$: (a) same pulses as in Fig. 2(a); (b) same pulses as in Fig. 2(b).

strength, pulse energy, channel spacing, and initial pulse separation), and we did a parallel study by using parameters derived from the NEC experiment. Figure 1(a) shows an incomplete collision between two DM solitons with $M = 10$, $\|u\|^2 = 94.3$ (corresponding to $\lambda = 5$, $\tau_{\mathrm{rms}} = 1.875$, and $\omega_{\mathrm{rms}} = 1.115$), and a channel separation $\Delta\Omega = 3.75$; the two pulses are separated initially by a distance $\Delta t_0 = 16$. Figure 1(b) shows the corresponding interaction when the pulses are initially placed at a much larger distance, $\Delta t_0 = 50$. In Fig. 1(a) the interaction results in the mutual destruction of the two pulses: that is, in collapse. The reason is that the DMNLS equation should be considered nonintegrable, and collapse is a typical nonintegrable effect (see, e.g., Ref. 24). From Fig. 1(b) we see that for a complete collision the collapse disappears, although the pulses still suffer from evident nonadiabatic effects. This scenario has been found to be valid for a rather large number of cases.

Note that [Fig. 1] collapse or significant nonadiabatic effects occur with relatively wide frequency separations (in our units, $\Delta\nu = 88$ GHz, i.e., 0.7 nm at 1550 μm). From either calculation it can be concluded that, should one try to carry out WDM soliton transmission with experimental configurations that correspond to these parameter values (or are even close to them), serious problems are likely to ensue.

Two comments should be made about the energy of the pulses in Fig. 1. The first comment is that the value of the energy is so large that these pulses would be unlikely to be used in practice, given the current output power limitations of the erbium-doped fiber amplifiers. However, it is well known that the energy required for obtaining a soliton with a given width τ_{rms} increases with the map strength: an effect called the energy enhancement[15,16,25] of dispersion-managed solitons. (Another way to look at this effect is to observe that, if one keeps the energy fixed instead, the pulse width increases with the map strength.) Therefore, to obtain DM pulses of acceptable width for communication purposes, one is forced to use larger values of energy as M increases. When the dispersion map is strong (i.e., for large values of M), the enhancement factor can be quite large, which explains why the energy of the pulses in Fig. 1 is so large.

The second comment is that one might be tempted to conclude incorrectly that the interaction properties are due only to the enhanced nonlinearity. If all other parameters are held fixed, higher energies lead to worse interaction behavior. However, if one fixes the pulse energy, all the other parameters of a DM soliton will depend on the map strength. Therefore the interaction properties also depend on the map strength, even if one keeps the pulse energy low. When the map strength M is large, as in the case of Fig. 1, serious nonadiabatic effects and spectral collapse can also occur at much lower energies.

To illustrate this last point, in Fig. 2 we present two incomplete WDM collisions for pulses at $M = 10$, with initial separation $\Delta t_0 = 16$ and dimensionless frequency separation $\Delta\Omega = 2$ (i.e., 0.38 nm at 1.55 μm in our units). Figure 2(a) refers to pulses with $\|u\|^2 = 15.58$ (yielding $\lambda = 2$, $\tau_{\mathrm{rms}} = 2.341$, and $\omega_{\mathrm{rms}} = 0.8747$), whereas Fig. 2(b) is relative to $\|u\|^2 = 4.276$ (yielding $\lambda = 1$, $\tau_{\mathrm{rms}} = 2.967$, and $\omega_{\mathrm{rms}} = 0.6790$). Note in particular that,

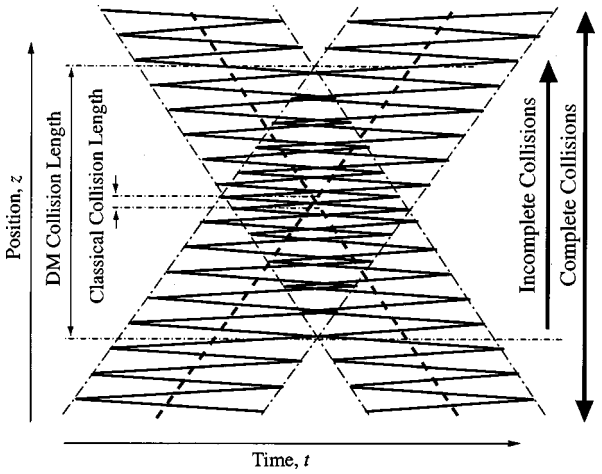

Fig. 4. Schematic diagram of a collision between DM pulses: dashed lines, the average trajectories of the pulses; solid lines, the actual trajectories. Also shown are the interaction lengths and the regions that correspond to complete and incomplete collisions.

even for Fig. 2(b), which corresponds to energy levels comparable with the energy of classical NLS solitons, one still observes nontrivial interaction effects. (Note, for example, the visible shift of the pulse mean time that takes place during the collision, the side humps after the collision, and the visible oscillations in the pulse amplitude before and after the collision.)

Thus, incomplete collisions with very strong dispersion maps can lead to serious nonadiabatic effects, even at large frequency separations or at moderate energies. As a consequence, these issues could represent an important constraint on the experimental design of soliton transmission systems. However, by proper choice of system parameters it is possible to obtain much more favorable configurations. For a given value of map strength, these parameters reduce to pulse energy and channel separation. For comparison, in Fig. 3 we show incomplete collisions of the same DM pulses as in Fig. 2 (same M and λ) with the same channel separation as in Fig. 1 (same $\Delta\Omega$). Here we see that, whereas in Fig. 3(a) nonadiabatic effects are still present, in Fig. 3(b) the interaction is almost indistinguishable from an elastic collision between NLS solitons.

7. INCOMPLETE COLLISIONS

To our knowledge, a formal definition of partial (or incomplete) collisions has never been given in the literature. In practice, we can characterize incomplete collisions as those collisions for which the final result depends on the initial pulse separation Δt_0 at $z = 0$ (or, equivalently, on the starting point z_0 if the pulses are set to collide at $z = 0$). Even for classical NLS solitons, it is well known that incomplete collisions induce permanent frequency shifts and lead to unacceptably large transmission penalties.[26] The main reason why incomplete collisions are intrinsically different from complete ones lies in the loss of symmetry in the overlap integral that yields the instantaneous frequency shift (see, e.g., Ref. 21), which in turn results in a net residual frequency shift even for pure NLS solitons.[27]

When dispersion management is present, the situation is further complicated by the large relative zigzags of the pulses, which have the consequence that the collision process starts much earlier than for classic solitons and continues for much longer distances. Figure 4 is a schematic diagram of a collision between strongly dispersion-managed pulses in different frequency channels. The relative temporal separation traveled by the pulses across each fiber segment is given by $2s\Delta\Omega$, which in practical cases can be quite large (cf. Fig. 4). As a consequence, the collision distance is increased severalfold.[10] In fact, unless

$$\Delta t_0 \geqslant 2s\Delta\Omega, \tag{11}$$

the pulses will start colliding soon after they are launched, and therefore the collision will be incomplete. Thus the difference between Figs. 1(a) and 1(b) is that inequality (11) is not satisfied for Fig. 1(a). In other words, when one is integrating NLS equation (1) with dispersion management, Fig. 1(a) must be regarded as an incomplete collision even though the pulses appear to be initially separated. This is so because the large relative zigzags of the pulses inside a dispersion map imply that the integration starts when the pulses are already colliding. In all our figures, these intermediate collisions are not visible because we are plotting the pulse profiles only stroboscopically at integer multiples of the map period, thus bypassing the large zigzags of the pulses.

Again, we emphasize that these results hold independently of whether one integrates the DMNLS equation or looks stroboscopically at integer multiples of the map period when integrating the NLS equation with dispersion management. Although the zigzags are not present in the DMNLS equation, the nonlocal term plays the role of an effective interaction potential, with the result that the DMNLS equation reproduces quite accurately the interaction properties of the DM solitons.

Finally, it is important to realize that collisions with initial separations such as the one used in Fig. 1 or smaller would be unavoidable in a dense WDM system because of the need to interleave several pulse trains (each in a different frequency channel) at the launch point in the fiber.

8. NEC REGIME

By properly choosing the system parameters, it is possible to find combinations that are quite favorable for WDM transmission. In our simulations, a particularly good combination was found when we based the choice of parameters on DM-soliton WDM transmission experiments recently performed by the NEC.[2,3] In this case, $M = 7.0$ and $\lambda = 0.578$, corresponding to $\|u\|^2 = 1.55$, $\tau_{\mathrm{rms}} = 3.717$, and $\omega_{\mathrm{rms}} = 0.540$.

Figure 5 shows an incomplete collision between NEC pulses with the same temporal and spectral separations as in Fig. 1(a). From Fig. 5(b) we can see that the frequency shifts and the small four-wave mixing contribution that one has for classical solitons—and even for pure

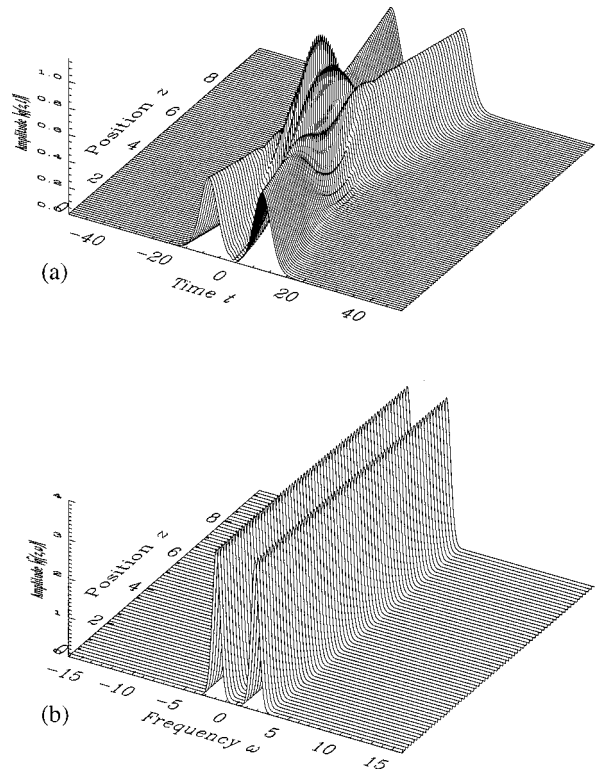

Fig. 5. Incomplete collision between NEC solitons with the same channel spacing and initial separation as in Fig. 1: (a) time domain, (b) frequency domain.

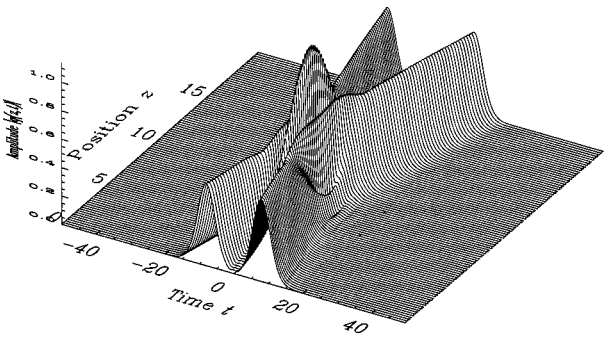

Fig. 6. Incomplete collision between NEC solitons with the same channel spacing and initial separation as in Fig. 2.

NLS solitons—effectively disappear (compare Fig. 5 with Figs. 1 and 2 of Ref. 23 and with Figs. 1–10 of Ref. 20). In fact, the collision-induced timing shift of the NEC pulses at 10 Mm smaller than the timing shift for a collision between pure NLS solitons with the same channel separation. Figure 6 shows an incomplete collision between NEC pulses with the same channel spacing and initial separation as in Fig. 2. For these pulses, nonadiabatic effects occur only at much smaller frequency separations, which are well below typical values used in WDM experiments.

It is worth noting that the NEC pulse profile is closer to Gaussian than the pulses in Fig. 1. A quantitative measure of this observation is provided by the time–bandwidth product, $\mathrm{TB} = \tau_{\mathrm{FWHM}}\nu_{\mathrm{FWHM}}$. The time–bandwidth product of NEC pulses is 0.406, which is closer to that of a Gaussian pulse (TB of 0.441) than that of the pulses in Fig. 1, for which the TB is 0.555. (For NLS solitons the TB is 0.315). As a final comment we recall that, for any given map strength, the expansion factor E is related to λ and thus to the pulse energy $\|u\|^2$. For NEC pulses, $E = 1.7$; for the pulses in Fig. 1, $E = 7.0$. [For the pulses in Fig. 2(a), $E = 5.1$; for those in Fig. 2(b), $E = 3.3$.] In general, our calculations indicate that larger values of λ (and therefore of E and $\|u\|^2$) tend to result in worse interaction behavior.

9. CONCLUSIONS

Dispersion-managed solitons are characterized by numerous design parameters that affect the overall properties of the system. Our results demonstrate that (i) different parameter ranges can lead to substantially different regimes with respect to WDM transmission of DM solitons; (ii) incomplete collisions are a special concern because they often lead to more-pronounced nonadiabatic effects; (iii) the interacting pulses can in some cases annihilate each other, a process called spectral collapse; and (iv) even when collapse is not present, serious nonadiabatic interaction effects are possible. In extreme cases, we found collapse or nonadiabatic effects even with large frequency separation or at low pulse energy. At the present time, a precise criterion that determines under which conditions the pulses will collapse has not been established; to do so remains a task for future research. In this context, however, the averaged DMNLS equation is particularly useful in as much as it represents a reduced model that retains the core properties of DM solitons. We hope that calculations such as these will provide indications of favorable parameter regimes for wavelength-division multiplexed dispersion-managed soliton transmission.

ACKNOWLEDGMENTS

We thank A. Hasegawa and W. L. Kath for many insightful discussions and T. Hirooka for providing valuable experimental data. We also thank one of the referees for a number of useful comments that helped us to improve the quality of the manuscript. This effort was partially sponsored by the National Science Foundation under grant ECS-9800152 and by the U.S. Air Force Office of Scientific Research, Air Force Materials Command, U.S. Air Force, under grant F49620-00-1-0031.

*Current address, Department of Engineering Sciences and Applied Mathematics, Northwestern University, Evanston, Illinois, 60208-3125; email address, biondini@northwestern.edu.

REFERENCES

1. D. LeGuen, S. DelBurgo, M. L. Moulinard, D. Grot, M. Henry, F. Favre, and T. Georges, "Narrow bank 1.02Tb/s (51 × 20 Gbit/s) soliton DWDM transmission over 1000 km of standard fiber with 100 km amplifier spans," in *Optical Fiber Communication Conference (OFC)*, 1999 OSA Techni-

cal Digest Series (Optical Society of America, Washington D.C., 1999), paper PD4.
2. K. Fukuchi, M. Kakui, A. Sasaki, T. Ito, Y. Inada, T. Tsuzaki, T. Shitomi, K. Fuji, S. Shikii, H. Sugahara, and A. Hasegawa, "1.1 Tb/s (55×20 Gb/s) dense WDM soliton transmission over 3020 km widely-dispersion-managed transmission line employing 1.55–1.58 μm hybrid repeaters," in *European Conference on Optical Communications* (Institute of Electrical Engineers, London, 1999), paper PD42.
3. T. Ito, K. Fukuchi, Y. Inada, T. Tetsufumi, M. Harumoto, M. Kakui, and K. Fuji, "3.2 Tb/s-1500 km WDM transmission experiment using 64 nm hybrid repeater amplifiers," in *Optical Fiber Communication Conference*, Vol. 38 of OSA Trends in Optics and Photonics Series (Optical Society of America, Washington, D.C., 2000), paper PD24.
4. A. Hasegawa, ed., *Massive WDM and TDM Soliton Transmission Systems* (Kluwer Academic, Dordrecht, The Netherlands, 2000).
5. V. E. Zakharov and S. Wabnitz, eds., *Optical Solitons: Theoretical Challenges and Industrial Perspectives* (Springer-Verlag, Berlin, 1999).
6. J. F. L. Devaney, W. Forysiak, A. M. Niculae, and N. J. Doran, "Soliton collisions in dispersion-managed wavelength-division-multiplexed systems," Opt. Lett. **22**, 1695–1697 (1997).
7. E. A. Golovchenko, A. N. Pilipetskii, and C. R. Menyuk, "Collision-induced timing jitter reduction by periodic dispersion management in soliton WDM transmission," Electron. Lett. **33**, 735–737 (1997).
8. H. Sugahara, A. Maruta, and Y. Kodama, "Optimal allocation of amplifiers in a dispersion-managed line for a wavelength-division multiplexed soliton transmission system," Opt. Lett. **24**, 145–147 (1999).
9. M. J. Ablowitz and G. Biondini, "Multiscale pulse dynamics in communication systems with strong dispersion management," Opt. Lett. **23**, 1668–1670 (1998).
10. P. V. Mamyshev and L. F. Mollenauer, "Soliton collisions in wavelength-division multiplexed dispersion-managed systems," Opt. Lett. **24**, 448–450 (1999).
11. D. J. Kaup, B. A. Malomed, and J. Yang, "Collision-induced pulse timing jitter in a wavelength-division-multiplexing system with strong dispersion management," J. Opt. Soc. Am. B **16**, 1628–1635 (1999).
12. Y. Chen and H. A. Haus, "Collisions in dispersion-managed soliton propagation," Opt. Lett. **24**, 217–219 (1999).
13. A. Hasegawa and Y. Kodama, *Solitons in Optical Communications* (Oxford University, New York, 1995).
14. I. R. Gabitov and S. K. Turitsyn, "Averaged pulse dynamics in a cascaded transmission system with passive dispersion compensation," Opt. Lett. **21**, 327–329 (1996).
15. N. J. Smith, N. J. Doran, F. M. Knox, and W. Forysiak, "Energy scaling characteristics of solitons in strongly dispersion-managed fibers," Opt. Lett. **21**, 1981–1983 (1996).
16. T.-S. Yang and W. L. Kath, "Analysis of enhanced-power solitons in dispersion-managed optical fibers," Opt. Lett. **22**, 985–987 (1997).
17. V. I. Petviashvili, "Equation of an extraordinary soliton," J. Plasma Phys. **2**, 257–258 (1976).
18. M. J. Ablowitz, G. Biondini, and E. S. Olson, "On the evolution and interaction of dispersion-managed solitons," in *Massive WDM and TDM Soliton Transmission Systems*, A. Hasegawa, ed. (Kluwer Academic, Dordrecht, The Netherlands, 2000), pp. 75–114.
19. C. Paré and P.-A. Bélanger, "Spectral domain analysis of dispersion management without averaging," Opt. Lett. **25**, 881–883 (2000).
20. M. J. Ablowitz, G. Biondini, S. Chakravarty, R. B. Jenkins, and J. R. Sauer, "Four-wave mixing in wavelength-division multiplexed soliton systems: ideal fibers," J. Opt. Soc. Am. B **14**, 1788–1794 (1997).
21. L. F. Mollenauer, S. G. Evangelides, and J. P. Gordon, "Wavelength division multiplexing with solitons in ultra-long distance transmission using lumped amplifiers," J. Lightwave Technol. **9**, 362–367 (1991).
22. P. V. Mamyshev and L. F. Mollenauer, "Pseudo-phase-matched four-wave mixing in soliton wavelength-division multiplexed transmission," Opt. Lett. **21**, 396–398 (1996).
23. M. J. Ablowitz, G. Biondini, S. Chakravarty, R. B. Jenkins, and J. R. Sauer, "Four-wave mixing in wavelength-division multiplexed soliton systems: damping and amplification," Opt. Lett. **21**, 1646–1648 (1996).
24. M. J. Ablowitz, M. D. Kruskal, and J. F. Ladik, "Solitary wave collisions," SIAM (Soc. Ind. Appl. Math.) J. Appl. Math. **36**, 428–437 (1979).
25. V. S. Grigoryan, T. Yu, E. A. Golovchenko, C. R. Menyuk, and A. N. Pilipetskii, "Dispersion-managed soliton dynamics," Opt. Lett. **22**, 1609–1611 (1997).
26. P. A. Andrekson, N. A. Olsson, J. R. Simpson, T. Tanbun-Ek, R. A. Logan, P. C. Becker, and K. W. Wecht, "Dependence of soliton interaction forces on wavelength separation in fibre amplifier based systems," Electron. Lett. **26**, 1499–1501 (1990).
27. Y. Kodama and A. Hasegawa, "Effect of initial overlap on the propagation of optical solitons at different wavelengths," Opt. Lett. **16**, 208–210 (1991).